

# Localization of the Adhesion Receptor Glycoprotein Ib-IX-V Complex to Lipid Rafts Is Required for Platelet Adhesion and Activation

Corie N. Shrimpton, Gautam Borthakur, Susana Larrucea, Miguel A. Cruz, Jing-Fei Dong, and José A. López

*Thrombosis Research Section, Department of Medicine, Baylor College of Medicine, Houston, TX 77030*

## Abstract

The platelet glycoprotein (GP) Ib-IX-V complex mediates the attachment of platelets to the blood vessel wall by binding von Willebrand factor (VWF), an interaction that also transmits signals for platelet activation and aggregation. Because the complex is extensively palmitoylated, a modification known to target proteins to lipid rafts, we investigated the role of raft localization in GP Ib-IX-V functions. In unstimulated platelets, a minor portion of the complex localized to Triton-insoluble raft fractions; this portion increased three to sixfold with platelet activation by VWF. Raft-associated GP Ib-IX-V was selectively palmitoylated, with GP Ib-IX-V-associated palmitate increasing in the raft fraction on VWF-mediated activation. The raft fraction was also the site of association between GP Ib-IX-V and the Fc receptor FcγRIIA. The importance of this association was demonstrated by the ability of the FcγRIIA antibody IV.3 to inhibit shear-induced platelet aggregation. Disruption of rafts by depleting membrane cholesterol impaired several GP Ib-IX-V-dependent platelet fractions: aggregation to VWF under static conditions and under shear stress, tyrosine phosphorylation, and adhesion to a VWF surface. Partial restoration of membrane cholesterol content partially restored shear-induced platelet aggregation and tyrosine phosphorylation. Thus, localization of the GP Ib-IX-V complex within rafts is crucial for both platelet adhesion and postadhesion signaling.

Key words: platelets • membrane microdomains • von Willebrand factor • cholesterol • signaling

## Introduction

When a blood vessel is injured, the first step in the hemostatic or thrombotic response is adhesion of platelets to exposed subendothelium. This reaction is mediated through an interaction of the platelet glycoprotein (GP)\* Ib-IX-V complex and subendothelial von Willebrand factor (VWF). The GP Ib-IX-V complex comprises four transmembrane polypeptide chains, GP Ib $\alpha$ , GP Ib $\beta$ , GP IX, and GP V, which are expressed on the platelet surface with a minimal stoichiometry of 2:2:2:1, respectively (1). The VWF-binding site is contained within a globular region at the NH<sub>2</sub> terminus of GP Ib $\alpha$  (for a review, see reference 1), the largest subunit of the complex.

Though initially believed to be simply an adhesive interaction, there is now considerable evidence to indicate that the binding of VWF to the GP Ib-IX-V complex results in the inside-out activation of the integrin  $\alpha_{IIb}\beta_3$ , and subsequent platelet aggregation (2–4). This receptor–ligand interaction has been shown to initiate a number of transmembrane signaling events including cytoskeletal reorganization (5), calcium mobilization (6), tyrosine phosphorylation of platelet proteins (7, 8), activation of phosphoinositide 3-kinase (9) and protein kinase C, and the synthesis of thromboxane A<sub>2</sub> (5). However, the precise pathway of signaling events induced by the GP Ib-IX-V–VWF interaction has yet to be defined.

One interesting modification of the GP Ib-IX-V complex that may provide a clue to its signaling function is the thiol acylation of GP Ib $\beta$  and GP IX by palmitate (10). Fatty acid modifications, such as palmitoylation, are believed to increase protein–lipid and protein–protein interactions, and thus may facilitate signal transduction. Indeed, palmitoylation has been shown to be important for protein

Address correspondence to J. López, Thrombosis Research Section, Dept. of Medicine, BCM 286, N1319, Baylor College of Medicine, One Baylor Plaza, Houston, TX 77030. Phone: 713-798-3470; Fax: 713-798-3415; E-mail: josel@bcm.tmc.edu

\*Abbreviations used in this paper: GP, glycoprotein; M $\beta$ CD, methyl- $\beta$ -cyclodextrin; MBS, MES-buffered saline; PRP, platelet-rich plasma; VWF, von Willebrand factor.

signaling functions (11, 12) and localization of signaling proteins to lipid rafts (12–15).

Lipid rafts (also known as GEMs, glycolipid-enriched membranes; DRMs, detergent-resistant membranes; and DIGs, detergent-insoluble glycolipid-rich domains) are dynamic assemblies of cholesterol and sphingolipids that are more ordered in structure than the rest of the plasma membrane (16). Rafts are specifically enriched in doubly acylated proteins such as the Src family kinases (17), transmembrane proteins modified by cysteine palmitoylation, such as the adaptor linker of T cell activation (12) and glycosylphosphatidylinositol-linked outer membrane proteins (18). Lipid rafts are believed to act as platforms for signal transduction by selectively attracting certain proteins while excluding others (for reviews, see references 19–21). These domains can be isolated from many cell types, including hematopoietic cells, where they have been shown to play critical roles in cell signaling (22–24).

Receptor clustering is an essential feature of signaling through lipid rafts. The clustering of raft components has been shown to result in the coalescence of the rafts (25), thus connecting raft proteins and accessory molecules into a larger domain, thereby facilitating signal transduction. Indeed, antibody-mediated cross-linking of the T cell antigen receptor (26) and Fc $\epsilon$ RI (27) has been shown to result in the aggregation of raft-associated proteins and in the initiation of signaling cascades that lead to immune cell signaling. Furthermore, cross-linking the raft component, ganglioside GM1, can also induce signaling (28).

Several lines of evidence have indicated that the cross-linking of GP Ib-IX-V complexes by VWF initiates signaling events that lead to platelet activation (29–33). Understanding signaling from the complex remains problematic, however, as none of its component polypeptides contain any of the classical domains involved in initiating signals. Nevertheless, VWF-induced cross-linking of multiple GP Ib-IX-V complexes may lead to receptor clustering, possibly incorporating other receptors into the clusters, and leading to their activation and the subsequent initiation of signaling pathways. Consistent with this, the GP Ib-IX-V complex has been shown to coimmunoprecipitate with the immunoregulatory tyrosine activation motif-containing proteins FcR  $\gamma$ -chain (34) and Fc $\gamma$ RIIA (35), and has been demonstrated to be physically associated with the later (35, 36) on the platelet surface. The similarities between signaling in immune cells through immune receptors and in platelets through the GP Ib-IX-V complex are intriguing, as is the fact that the complex is palmitoylated. Therefore, we speculated that lipid rafts might play a key role in signaling after engagement of the complex by VWF. Here, we report on the association of the GP Ib-IX-V complex with lipid rafts and present evidence for a physiological role for this association in GP Ib-IX-V-mediated platelet function.

## Materials and Methods

**Materials.** The following mAbs, unlabeled and FITC-conjugated, were obtained from commercial sources: AK2 (anti-GP

Ib $\alpha$ ; Research Diagnostics); IV.3 (anti-Fc $\gamma$ RIIA; Mederex); 4D10.1 (anti-Syk) and 4G10 (antiphosphotyrosine) were from Upstate Biotechnology; SZ2 (anti-GP Ib $\alpha$ ); and P2 (anti- $\alpha$ <sub>IIb</sub> $\beta$ <sub>3</sub>) were purchased from Beckman Coulter. WM23 (anti-GP Ib $\alpha$ ) and purified human VWF were provided by M.C. Berndt (Baker Medical Research Institute, Melbourne, Australia). Polyclonal antisera generated against  $\alpha$ <sub>IIb</sub> $\beta$ <sub>3</sub> and the mAb (AP3) against the  $\beta$ <sub>3</sub> integrin were provided by P. Thiagarajan (VA Medical Center, Houston, TX) and P. Newman (Blood Research Institute, Milwaukee, WI), respectively. Rabbit anti-mouse IgG was from Zymed Laboratories. Secondary antibody for immunoblotting and chemiluminescence detection reagents were from Pierce Chemical Co. Nitrocellulose was from Bio-Rad Laboratories. Pansorbin, a suspension of heat-killed *Staphylococcus aureus* cells, was from Calbiochem. *n*-Octyl  $\beta$ -D-glucopyranoside was from Fisher Scientific. [9,10-<sup>3</sup>H-(N)]palmitic acid was from Perkin Elmer Life Science. Na<sup>125</sup>I was from ICN. Citrated porcine blood was provided by M. Schreiber (Baylor College of Medicine, Houston, TX) and plasma was obtained by sequential centrifugation as described below for the isolation of human platelets. Methyl- $\beta$ -cyclodextrin (M $\beta$ CD) and cholesterol-loaded M $\beta$ CD were purchased from Sigma-Aldrich, as were all other reagents unless otherwise stated.

**Platelet Preparation.** Human blood was drawn from healthy, medication-free, donors into 1/9 volume of 3.8% sodium citrate. Platelet-rich plasma (PRP) was obtained by centrifugation (160 g, 20 min, 25°C). Platelets were obtained by subsequent centrifugation of the PRP (800 g, 12 min, 25°C) in the presence of 300 nM prostacyclin to prevent aggregation. If washed platelets were desired, blood was collected into 1/6 volume of acid-citrate-dextrose (85 mM trisodium citrate, 71 mM citric acid, and 111 mM dextrose). Platelets were obtained as described above, with the omission of prostacyclin, and were washed by resuspension in CGS buffer (13 mM sodium citrate, 30 mM glucose, and 120 mM NaCl), centrifuged again, and resuspended to their original PRP volume in buffer 1 (134 mM NaCl, 12 mM NaHCO<sub>3</sub>, 2.9 mM KCl, 0.34 mM Na<sub>2</sub>HPO<sub>4</sub>, 1 mM MgCl<sub>2</sub>, 10 mM Hepes, 5 mM glucose, and 0.3 g/100 ml A; reference 37). To ensure that observations were not restricted to an individual platelet donor, all experiments were repeated several times using blood from different donors.

**Platelet Lysis and Sucrose Density-Gradient Fractionation.** Platelets (2–3  $\times$  10<sup>8</sup>/ml; 4 ml) prepared as described above, were lysed with 2 ml ice-cold Triton X-100 lysis buffer (25 mM MES, pH 6.5, 150 mM NaCl, 1% [wt/vol] Triton X-100, 10 mM benzamidine, 1 mM PMSF, 20  $\mu$ g/ml aprotinin, 20  $\mu$ g/ml leupeptin, and 100  $\mu$ g/ml soybean trypsin inhibitor). All subsequent steps were performed at 4°C. The lysate was adjusted to 40% (wt/vol) sucrose by the addition of an equal volume of 80% (wt/vol) sucrose in MES-buffered saline (25 mM MES, pH 6.5, 150 mM NaCl). 4 ml of 30% sucrose, followed by 2 ml of 5% sucrose, were gently layered over the 40% sucrose fraction in an ultracentrifuge tube. The samples were then centrifuged at 200,000 g at 4°C for 18 h in a SW40 rotor (Beckman Coulter). 12 equal fractions were collected from the top of the gradient.

**Immunoprecipitation and Immunoblotting.** Equal volumes of each fraction collected from the sucrose gradient were precleared for 1 h at 4°C with Pansorbin. After removing the Pansorbin by centrifugation, the samples were incubated overnight with primary antibodies and then immunoprecipitated with Pansorbin or by the sequential addition of rabbit anti-mouse IgG and Pansorbin when a primary mAb was used. The Pansorbin was pelleted by centrifugation, washed three times, and the bound protein eluted by boiling in 2 $\times$  sample buffer containing 2%

$\beta$ -mercaptoethanol. Control immunoprecipitations were performed with normal mouse IgG and/or rabbit anti-mouse IgG alone. Immunoprecipitated proteins were resolved by 10% SDS-PAGE under reducing conditions and transferred to nitrocellulose for Western blotting/ECL. Dot blots were performed using a Bio-Dot Microfiltration Apparatus (Bio-Rad Laboratories) according to the manufacturer's instructions and probed for ganglioside GM1 with HRP-conjugated cholera toxin B subunit (10  $\mu$ g/ml).

**$^3$ H]Palmitate Labeling of Platelet Proteins.** Washed platelets were incubated at 37°C with 20  $\mu$ Ci [9,10- $^3$ H-(N)]palmitic acid for 45 min. Platelets were washed to remove unincorporated radioactivity and then activated with 10% (vol/vol) porcine plasma (as a source of VWF). Platelets were pelleted, fractionated by sucrose gradient centrifugation as described above. *n*-Octyl  $\beta$ -D-glucopyranoside (60 mM) was added to each fraction to ensure solubilization of the lipid rafts and associated proteins. The GP Ib complex was immunoprecipitated (SZ2) from each fraction and the associated radioactivity counted in a  $\gamma$ -counter.

**Cholesterol Depletion and Repletion of Platelets.** To specifically deplete the platelet membrane of cholesterol, PRP was incubated with M $\beta$ CD in buffer 1 at a final concentration of 10 mM (or with an equal volume of buffer 1 as a control) for 30 min at 37°C. The platelets were then used in subsequent experiments. For cholesterol repletion studies, cholesterol-depleted platelets were centrifuged and resuspended in buffer 1 containing 3 mM cholesterol-loaded M $\beta$ CD and incubated for 30 min at 37°C. Platelets were centrifuged and resuspended in fresh platelet-poor plasma.

**Platelet Aggregometry.** Platelet aggregation experiments using PRP were performed with constant stirring at 1,200 rpm at 37°C in a four-channel aggregometer (Biodata Corp.). After cholesterol depletion of the platelets as described above, aggregation was initiated by the addition of either ristocetin (1 mg/ml) or 10% (vol/vol) porcine plasma.

**Shear-induced Platelet Aggregation.** Control or cholesterol-depleted platelets (PRP; 500  $\mu$ l) were loaded onto a cone-plate viscometer (Rheostress 1 CS Rheometer; Haake) and sheared for 1 min at 10,000 1/s. 10  $\mu$ l of sheared PRP was collected and fixed in an isotonic solution containing 0.1% glutaraldehyde before analysis. The extent of platelet aggregation was determined by particle counting in a Coulter Counter (Coulter). The lower the particle count, the greater the extent of aggregation. In studies examining the contribution of Fc $\gamma$ RIIA to shear-induced platelet aggregation, control platelets were incubated with 25  $\mu$ g/ml of IV.3, AK2, or abciximab for 10 min at room temperature before shear. To study the effect of cholesterol depletion on shear-induced tyrosine phosphorylation, washed, untreated, cholesterol-depleted and cholesterol-depleted/repleted platelets were subject to shear before lysis in 2 $\times$  sample buffer containing 2%  $\beta$ -mercaptoethanol and analysis by SDS-PAGE.

**Platelet Adhesion Assays in a Parallel-Plate Flow Chamber.** Recombinant VWF A1 domain (amino acids 479–717; the domain interacting with GP Ib $\alpha$ ) was expressed and purified as described previously (38). The protein (diluted to 150  $\mu$ g/ml with TBS) was immobilized onto glass coverslips by incubation at 37°C for 1 h. A coated coverslip was then incorporated into a parallel-plate flow chamber (Glycotech) so that it formed the lower surface of the chamber. The flow chamber was then mounted onto an inverted stage microscope (Eclipse TE300; Nikon Inc.) equipped with an image recording system. PRP was incubated with M $\beta$ CD as described above before perfusion through the chamber at a flow rate of 0.6 ml/min, generating a wall shear rate of 1,500 1/s.

**Binding of  $^{125}$ I-labeled WM23 to Platelets.** The GP Ib $\alpha$ -specific mAb WM23 was iodinated using the Chloramine T method

(39) and separated from free label by gel filtration on Sephadex G25.  $^{125}$ I-WM23 (10  $\mu$ g/ml) was incubated with PRP for 20 min at room temperature; the platelets were then washed, resuspended with buffer 1, and either left untreated or activated with 10% (vol/vol) porcine plasma or 10  $\mu$ M ADP. Lysis and sucrose gradient fractionation was performed as above and the radioactivity associated with each fraction determined in a  $\gamma$ -counter.

**Binding of  $^{125}$ I-labeled VWF to Platelets.** Untreated or cholesterol-depleted washed platelets (final concentration  $5 \times 10^7$ /ml, in TBS/0.1% BSA) were incubated with increasing concentrations of  $^{125}$ I-VWF (iodinated as for WM23) for 30 min at room temperature in the presence of ristocetin (1 mg/ml). The samples were centrifuged at 20,000 *g* for 2 min and the supernatant removed. The radioactivity associated with the pellet was measured in a  $\gamma$ -counter. Nonspecific binding was determined by including 10  $\mu$ g/ml of the inhibitory anti-GP Ib $\alpha$  mAb AK2 in a parallel assay.

**Flow Cytometry.** After treatment with M $\beta$ CD, PRP (10  $\mu$ l) was incubated with 30  $\mu$ l buffer 1 containing 10  $\mu$ l of either FITC-conjugated anti-GP Ib (SZ2) or anti- $\alpha_{IIb}\beta_3$  (P2) mAbs. After a 20-min incubation at room temperature, the samples were diluted 20-fold with PBS and analyzed in an EPICS XL Coulter Flow Cytometer (Coulter). Background binding was determined from parallel samples incubated with FITC-conjugated mouse IgG.

## Results

**A Fraction of the GP Ib-IX-V Complex Resides within Lipid Rafts.** Doherty et al. (40) described previously the presence of platelet GP Ib $\alpha$  in rafts, but did not characterize this further. Because of our interest in the signaling functions of the GP Ib-IX-V complex, and because of the conspicuous presence of palmitate on two of its subunits, we investigated the role of raft localization in GP Ib-IX-V complex function. On sucrose density fractions of 1% Triton X-100 platelet lysates, a significant portion of the GP Ib-IX-V complex could be found in the early fractions (fractions 3–5), as determined by immunoprecipitation and immunoblotting for GP Ib $\alpha$  (Fig. 1 A, top). Upon platelet activation with ristocetin/human VWF, the amount of GP Ib-IX-V complex in these fractions increased approximately threefold (Fig. 1 A, middle). We confirmed that the GP Ib-IX-V complex found in the early fractions was localized in lipid rafts by staining the fractions for the raft marker ganglioside GM1, which also appeared predominantly in fractions 3–5 (Fig. 1 B, third panel). Concomitant measurement of the total protein content of the fractions indicates that fractions 3–5 contained only 1–2% of the total protein (unpublished data). The localization of the complex in lipid rafts was not an artifact of Triton X-100 solubilization, as we observed similar localization to raft fractions when the platelets were lysed in two other non-ionic detergents, Brij 58 and Brij 46 (unpublished data). We also sought to confirm the increased localization of the GP Ib-IX-V complex to the raft fraction upon VWF activation of platelets by other means. Therefore, we examined the effect of platelet activation with porcine VWF on the localization of an iodinated anti-GP Ib $\alpha$  mAb. The antibody, WM23, binds within a mucin-like domain separating the ligand-binding domain from the plasma membrane

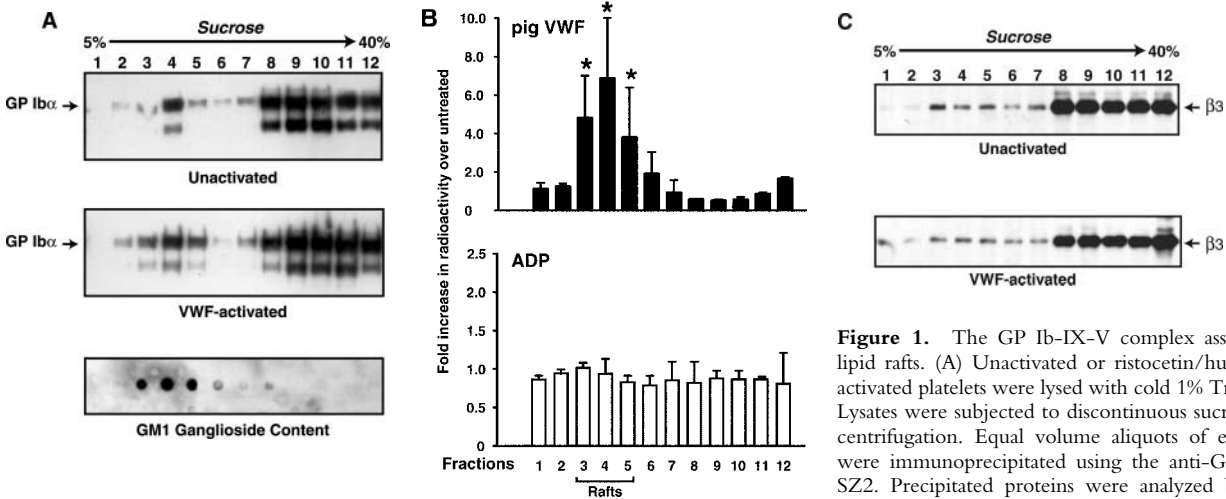


**Figure 1.** The GP Ib-IX-V complex associates with lipid rafts. (A) Unactivated or ristocetin/human VWF-activated platelets were lysed with cold 1% Triton X-100. Lysates were subjected to discontinuous sucrose gradient centrifugation. Equal volume aliquots of each fraction were immunoprecipitated using the anti-GP Ib $\alpha$  mAb SZ2. Precipitated proteins were analyzed by reducing SDS-PAGE followed by Western blot analysis with an anti-GP Ib $\alpha$  mAb (WM23). Band intensities were quantitated by scanning densitometry. Blots represent seven independent experiments. The position of the lipid rafts was identified by dot blotting of GM1 using HRP-conjugated cholera toxin B subunit as a probe. The lipid raft fraction floats within sucrose gradient fractions 3–5. (B) Platelets, prelabeled with  $^{125}\text{I}$ -WM23, were left untreated or activated with either porcine VWF or ADP before being lysed and subjected to sucrose gradient centrifugation. The data represent the fold-increase in radioactivity on VWF-induced platelet activation, compared with unactivated platelets ( $n = 3$ ,  $\pm$ SEM). (C) Unactivated or porcine VWF-activated platelets were lysed and subjected to sucrose gradient centrifugation. Equal-volume aliquots of each fraction were immunoprecipitated using polyclonal antisera against  $\alpha_{\text{IIb}}\beta_3$ . Precipitated proteins were analyzed by reducing SDS-PAGE followed by Western blot analysis with an anti- $\beta_3$  integrin mAb (AP3). The blots are representative of three independent experiments.

and does not affect ligand binding. The platelets were pretreated with  $^{125}\text{I}$ -labeled antibody, and lysed in their resting state, or after activation with porcine VWF. Porcine VWF is known to bind human GP Ib $\alpha$  without requiring modulators or shear stress, and to activate platelets (41, 42). Fig. 1 B shows the fold changes in antibody-associated radioactivity as a consequence of platelet activation with either porcine VWF (top panel) or ADP (bottom panel). The amount of radioactivity associated with the raft fractions increased three to sixfold upon platelet activation with porcine VWF and diminished correspondingly in the latter fractions (Fig. 1 B, top). This increase occurred with platelet activation by VWF, but not in platelets activated with ADP (Fig. 1 B, bottom).

To determine whether activation produced a general increase in the raft localization of platelet adhesive receptors, we also examined  $\alpha_{\text{IIb}}\beta_3$  distribution in the sucrose density fractions from lysates of unstimulated platelets and platelets activated with VWF. In unstimulated platelets, a small fraction of the total  $\alpha_{\text{IIb}}\beta_3$  migrated in the early fractions (Fig. 1 C, top), but the quantity of  $\alpha_{\text{IIb}}\beta_3$  in these fractions did not increase with VWF-induced platelet activation (Fig. 1 C, bottom).

**Lipid Raft Associated GP Ib-IX-V Complex Is Palmitoylated.** Within the GP Ib-IX-V complex, both GP Ib $\beta$  and GP IX are palmitoylated at cysteinyl residues proximal to the cytoplasmic face of the plasma membrane (10). Given the proposed stoichiometry of the complex, in its minimal conformation and fully palmitoylated state one would expect four palmitate moieties per complex, leading us to consider that the complex may indeed localize to lipid rafts through this fatty acyl modification. Therefore, we evaluated whether the fraction of the GP Ib-IX-V complex re-

siding in rafts was selectively palmitoylated. Platelets were labeled with  $^3\text{H}$ palmitate before being lysed and fractionated in a sucrose density gradient. The GP Ib-IX-V complex was immunoprecipitated from each fraction, in the presence of octyl- $\beta$ -glucopyranoside to exclude associated palmitate-containing lipids, and the radioactivity of the immunoprecipitate was counted. Approximately half of the total GP Ib-IX-V complex-associated palmitate in unstimulated platelets was localized to the raft fractions (Fig. 2 A) with the complex-associated palmitate being approximately fourfold greater in fraction 4 than in fraction 10, a fraction that contains approximately twice the absolute quantity of GP Ib-IX-V in fraction 4 (Fig. 1 A). This result strongly suggests that palmitoylation of the complex is responsible for its partitioning to rafts. As expected, binding of porcine VWF to the complex was associated with an increase in palmitoylated GP Ib-IX-V complex in the raft fraction, but not in nonraft fractions (Fig. 2 B).

**Raft Disruption by Cholesterol Depletion Inhibits GP Ib-IX-V-mediated Platelet Function.** Then we investigated the physiological significance of the partitioning of the GP Ib-IX-V complex to lipid rafts. Membrane cholesterol depletion is now an established method of disrupting lipid rafts and raft-associated functions (20). In these studies, we selectively depleted platelet membrane cholesterol using the cholesterol-binding agent M $\beta$ CD (43). As a prelude to functional studies, we examined the cholesterol removal by M $\beta$ CD from platelets. 10 mM M $\beta$ CD efficiently removes cholesterol from  $^3\text{H}$ cholesterol-labeled platelets as a function of time, with  $\sim$ 75% of the incorporated cholesterol released after 30 min. Treatment of platelets with M $\beta$ CD resulted in a complete loss of GP Ib-IX-V from the raft fractions from the lipid raft fractions (Fig. 3 A).

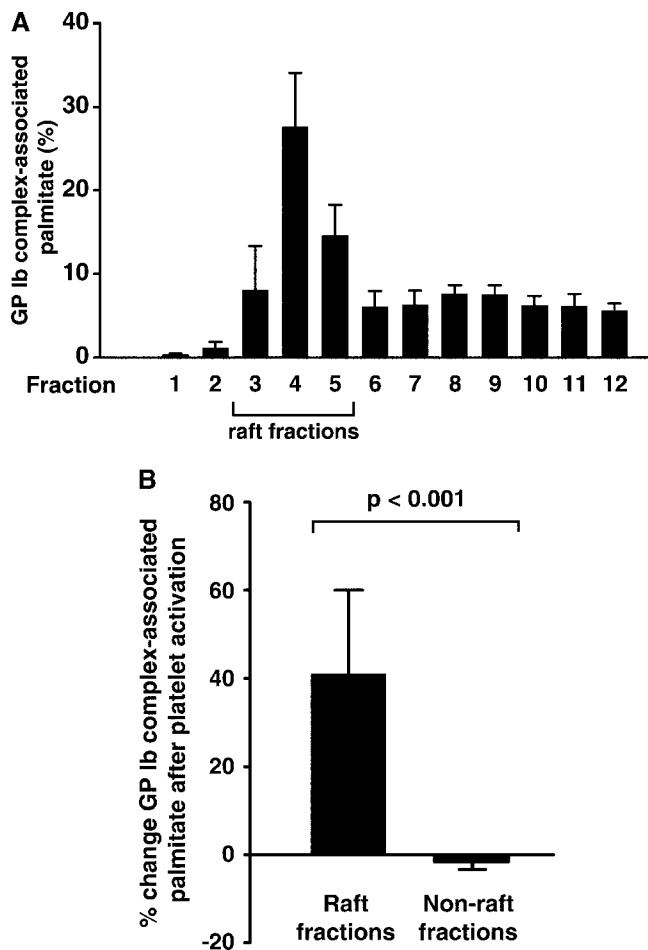


**Figure 2.** Raft-associated GP Ib-IX-V complex is selectively palmitoylated. Unactivated or porcine VWF-activated [ $^3\text{H}$ ]palmitate-labeled platelets were lysed with 1% Triton X-100. Lysates were subjected to discontinuous sucrose gradient centrifugation. Equal-volume aliquots of each fraction were immunoprecipitated using an anti-GP Ib $\alpha$  mAb (SZ2) and the associated radioactivity counted in a  $\gamma$ -counter. (A) Percentage of total GP Ib-associated [ $^3\text{H}$ ]palmitate by fraction from unactivated platelets ( $n = 5$ ,  $\pm$ SEM). (B) Percentage change of total GP Ib-associated [ $^3\text{H}$ ]palmitate upon activation in raft fractions (3–5) and nonraft fractions (1–2, 6–12) ( $n = 3$ ,  $\pm$ SEM).

Next we examined the effect of cholesterol depletion on VWF-induced platelet aggregation, under both static conditions and in the presence of shear stress. Aggregation induced by ristocetin/human VWF or porcine VWF (Fig. 3 B) was inhibited by  $\sim 70\%$  by cholesterol depletion. Moreover, cholesterol depletion significantly inhibited shear-induced aggregation (Fig. 3 C). The inhibitory effects of cholesterol depletion were both time- and M $\beta$ CD dose-dependent (unpublished data) with the inhibitory effect correlating with the degree of cholesterol depletion. To ensure that the results observed with cholesterol depletion were not secondary to a nonspecific toxic effect of M $\beta$ CD treatment, we performed control experiments in which we partially reconstituted membrane cholesterol by treating cholesterol-depleted platelets with cholesterol-loaded M $\beta$ CD. Adding cholesterol back partially restored shear-induced

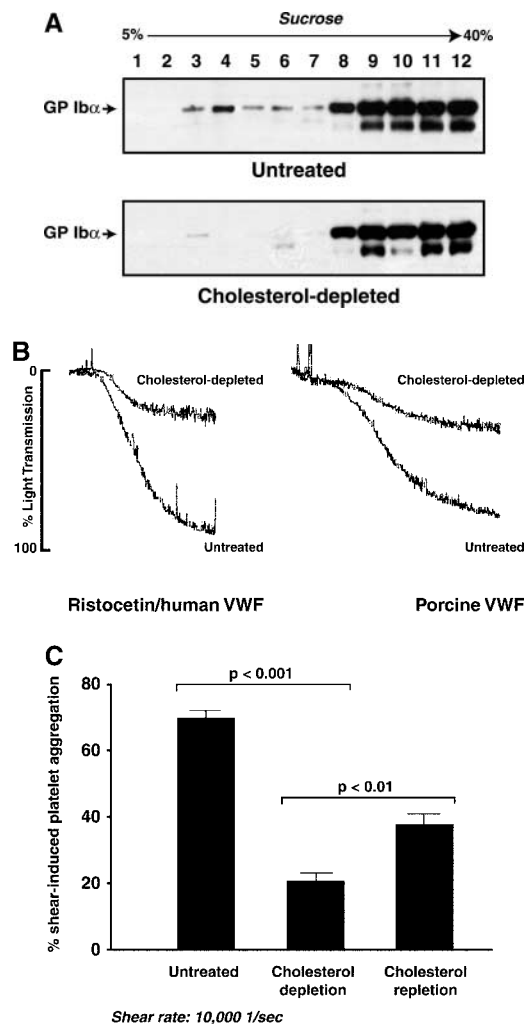


**Figure 3.** Cholesterol depletion results in the dissociation of the GP Ib-IX-V complex from the lipid raft fraction and inhibits GP Ib-mediated platelet activation. (A) Untreated or cholesterol-depleted platelets were lysed and subjected to sucrose gradient centrifugation. Equal-volume aliquots of each fraction were immunoprecipitated using an anti-GP Ib $\alpha$  mAb (SZ2). Precipitated proteins were analyzed by reducing SDS-PAGE followed by Western blot analysis with an anti-GP Ib $\alpha$  mAb (WM23). Blot is representative of five independent experiments. (B) Aggregation of untreated or cholesterol-depleted platelets induced by ristocetin/human VWF or porcine VWF. Aggregation was by conventional light aggregometry. Data are representative of five independent experiments. (C) Untreated, cholesterol-depleted, and cholesterol-depleted/repleted platelets were sheared in a cone-plate viscometer for 60 s at 10,000 1/s. After shear, an aliquot was fixed and the extent of platelet aggregation was determined by particle counting in a Coulter counter. The data represent the mean  $\pm$ SEM of triplicate samples from two independent experiments.

aggregation, albeit not to the levels seen before the platelets were treated with M $\beta$ CD (Fig. 3 C).

These results suggested a role for lipid rafts in GP Ib-IX-V signaling functions. We examined signaling function directly by determining the effect of cholesterol depletion with M $\beta$ CD on tyrosine phosphorylation induced during platelet activation with porcine VWF. M $\beta$ CD-treated platelets demonstrated a marked delay in the time course of phosphorylation of several proteins, among them the ty-

rosine kinase Syk, which has been implicated in the signaling pathways activated by VWF binding to platelets (Fig. 4 A). We observed a similar effect of cholesterol depletion on the phosphorylation of Syk associated with shear-induced platelet aggregation (Fig. 4 B). As with aggregation, cholesterol repletion largely restored shear-induced Syk phosphorylation.

*The GP Ib-IX-V Complex Colocalizes with FcγRIIA in Lipid Rafts.* Several lines of evidence indicate that the GP Ib-IX-V complex is physically and functionally associated with the immunoregulatory tyrosine activation motif-containing platelet Fc receptor FcγRIIA. Several different techniques have demonstrated that the receptors physically associate (35, 36), and antibodies to either receptor can block the binding of ligands of the other (35, 44). In addition, FcγRIIA has been implicated in the transmission of a portion of the signals generated on VWF binding to the GP Ib-IX-V complex (44, 45). Given that the complex is present in vast excess to FcγRIIA on the platelet surface (1), we examined whether association of the two receptors was confined to raft domains. We immunoprecipitated FcγRIIA from the sucrose gradient fractions and evaluated the precipitate by immunoblotting

with the anti-GP Ibα mAb WM23 (Fig. 5 A). Association of the two proteins occurred almost exclusively in the rafts, supporting the hypothesis that GP Ib-IX-V induced signal transduction may be mediated, at least in part, by FcγRIIA. We observed no change in the extent of association between the two proteins after platelet activation by porcine VWF. Of interest, as with the GP Ib-IX-V complex, only a portion of FcγRIIA resides in the raft fraction (Fig. 5 A, bottom), but it is this fraction that contributes virtually all of the FcγRIIA that associates with the GP Ib-IX-V complex.

We also examined the functional implications of FcγRIIA association with the GP Ib-IX-V complex in the raft fractions by assessing the effect of the FcγRIIA mAb IV.3 on shear-induced platelet aggregation. When preincubated with a platelet suspension before shearing, IV.3 markedly inhibited shear-induced platelet aggregation (60% inhibition), whereas a control antibody had no effect (Fig. 5 B). Aggregation was completely inhibited by antibodies against either GP Ibα or the α<sub>IIb</sub>β<sub>3</sub> complex, as expected for a pathway involving first the binding of VWF to GP Ibα and subsequent activation α<sub>IIb</sub>β<sub>3</sub> and platelet aggregation.

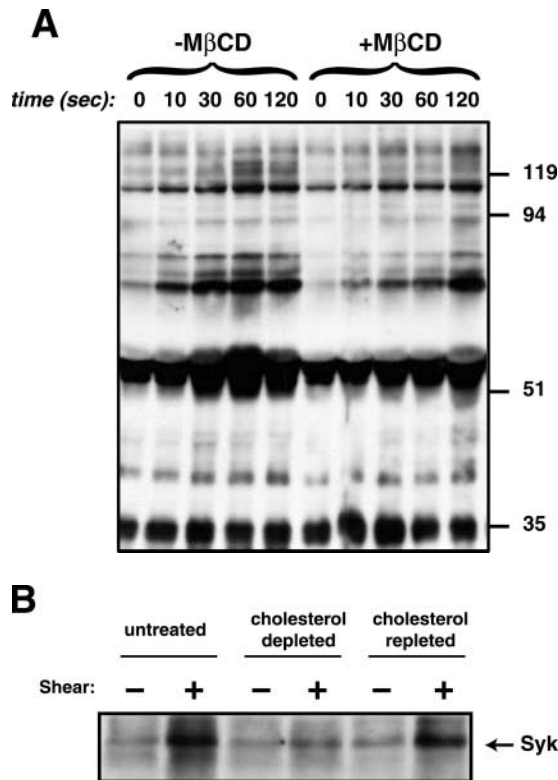


**Figure 4.** Cholesterol depletion results in decreased VWF-stimulated tyrosine phosphorylation. (A) Washed untreated or cholesterol-depleted platelets were sheared in a cone-plate viscometer for the indicated times at 10,000 1/s before lysis and direct analysis of total protein tyrosine phosphorylation by SDS-PAGE and western with mAb 4G10. (B) Tyrosine phosphorylation status of Syk before and after shear (60 s at 10,000 1/s) in untreated, cholesterol-depleted or cholesterol-depleted/repleted platelets. This figure is representative of three independent experiments

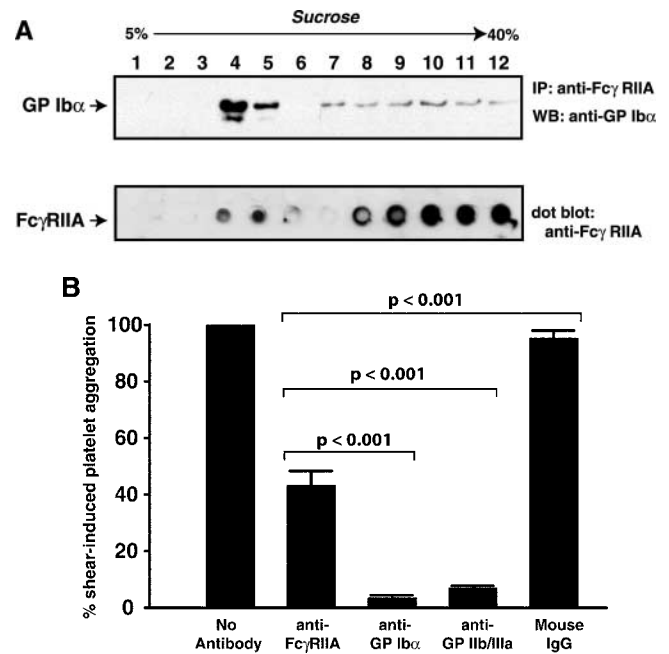


**Figure 5.** Colocalization of the GP Ib-IX-V complex and FcγRIIA in lipid rafts. (A) Unactivated platelets were lysed and subjected to sucrose gradient centrifugation. Equal-volume aliquots of each fraction were immunoprecipitated using an anti-FcγRIIA mAb (IV.3). Precipitated proteins were analyzed by reducing SDS-PAGE followed by Western blot analysis with WM23 (top). The distribution of total FcγRIIA across the gradient was determined by dot blotting with IV.3 (bottom). Blots represent three independent experiments. (B) PRP was preincubated without antibody or with anti-FcγRIIA mAb (IV.3), anti-GP Ib mAb (AK2), anti-α<sub>IIb</sub>β<sub>3</sub> (abciximab), or mouse IgG for 10 min before shearing in a cone-plate viscometer for 60 s at 10,000 1/s. After shearing the sample, an aliquot was fixed and the extent of platelet aggregation was determined by particle counting using a Coulter counter ( $n = 10$ , mean  $\pm$  SEM).

*Cholesterol Depletion Markedly Inhibits GP Ib-IX-V-mediated Adhesion of Platelets to a VWF Surface Under Conditions of Flow.* Also we investigated the effect of cholesterol depletion on GP Ib-IX-V-mediated platelet adhesion to a surface of immobilized VWF A1 under flow. We perfused untreated or M $\beta$ CD-treated platelets over a matrix of purified recombinant VWF A1 domain, a fragment of VWF containing the GP Ib $\alpha$  binding site and capable of supporting platelet adhesion (Fig. 6; reference 38). Use of the A1 domain allowed us to restrict our analysis to the effect of cholesterol depletion on GP Ib-IX-V complex-mediated platelet adhesion, as the A1 domain lacks binding sites for other platelet adhesion receptors. Treatment of the platelets with M $\beta$ CD markedly inhibited their ability to adhere to the A1 surface at both high (1,500 1/s) and low (300 1/s) shear stresses (unpublished data).

*Cholesterol Depletion Alters Neither GP Ib-IX-V Complex Conformation, Receptor Levels, nor the Binding of Soluble VWF Under Static Conditions.* To exclude the possibility that the loss of platelet function observed after cholesterol depletion was due to a conformational alteration in GP Ib-IX-V or to its loss from the platelet surface, we assessed receptor levels and VWF binding. The surface expression of the GP Ib-IX-V complex and of the integrin  $\alpha_{IIb}\beta_3$  on cholesterol-depleted platelets was determined by flow cytometry after surface labeling of these receptors with FITC-conjugated mAbs (Fig. 7 A). Surface levels of these receptors remained unchanged after a 30-min treatment with 10 mM M $\beta$ CD. In addition, the extent of ristocetin-induced binding of  $^{125}$ I-VWF, over a range of VWF concentrations, was equivalent in the untreated and cholesterol-depleted platelet samples (Fig. 7 B).

## Discussion

In this paper, we provide evidence for a role for lipid rafts in GP Ib-IX-V-mediated platelet function. We have demonstrated that a subset of the GP Ib-IX-V complex is constitutively associated with lipid rafts in unstimulated platelets and is further recruited to these membrane micro-

domains upon stimulation by VWF. By the techniques employed here, only a minor fraction of the complex localizes to the raft fractions, but this fraction seems to have a crucial role in the functions of the complex. Disruption of rafts by cholesterol depletion markedly inhibited virtually every aspect of GP Ib-IX-V complex function, from its ability to mediate platelet aggregation after binding VWF under static conditions, to shear-induced platelet aggregation, to its function in mediating platelet adhesion under flow. Impairment of the former two functions appeared to involve interference with the signaling functions of the complex, as in both cases cholesterol depletion of platelets resulted in diminished tyrosine phosphorylation (Fig. 4). Partial repletion of platelet cholesterol restored both shear-induced platelet aggregation (Fig. 3 C) and shear-induced phosphorylation of the tyrosine kinase Syk (Fig. 4 B), a downstream effector of GP Ib-IX-V-initiated signaling. It is difficult to gauge whether the extent of restoration of platelet membrane cholesterol was complete, but this is unlikely, possibly accounting for the incomplete restoration of GP Ib-IX-V functions. This would be consistent with our observation that the effects of M $\beta$ CD treatment on platelet function were dose and time-dependent (unpublished data). It is also possible that extensive manipulation of the platelets through the prolonged incubations required to first deplete the cholesterol and then add it back may have itself blunted their responsiveness.

As for the effect of cholesterol depletion on platelet adhesion under conditions of flow, this effect appears to be independent of GP Ib-IX-V complex signaling. The initial step in platelet adhesion under high shear stresses involves the tethering of the platelets to a VWF surface, which precedes any signals transmitted from the GP Ib-IX-V complex. The GP Ib-IX-V-VWF interaction then allows the platelets to decelerate by rolling, enabling the engagement of other receptors that aid in the activation of the platelets and their firm adhesion. In our studies of adhesion, we excluded participation of other receptors and therefore any confounding effects of cholesterol depletion on these receptors by using the VWF A1 domain, which contains a

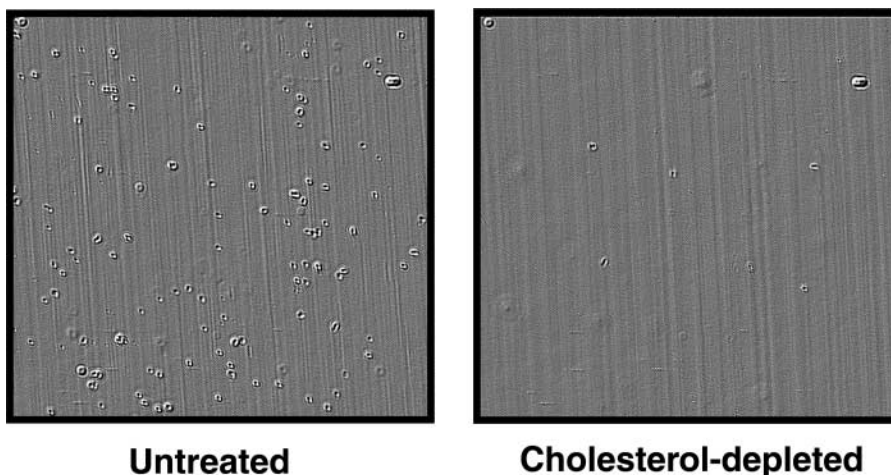


**Figure 6.** Cholesterol depletion inhibits platelet adhesion to immobilized VWF-A1 domain. Glass coverslips were coated with VWF A1 domain (150  $\mu$ g/ml) and perfused with plasma containing untreated or cholesterol-depleted platelets, at a shear rate of 1,500 1/s. The embossed micrographs represent five independent assays. Original magnification: 400 $\times$ .

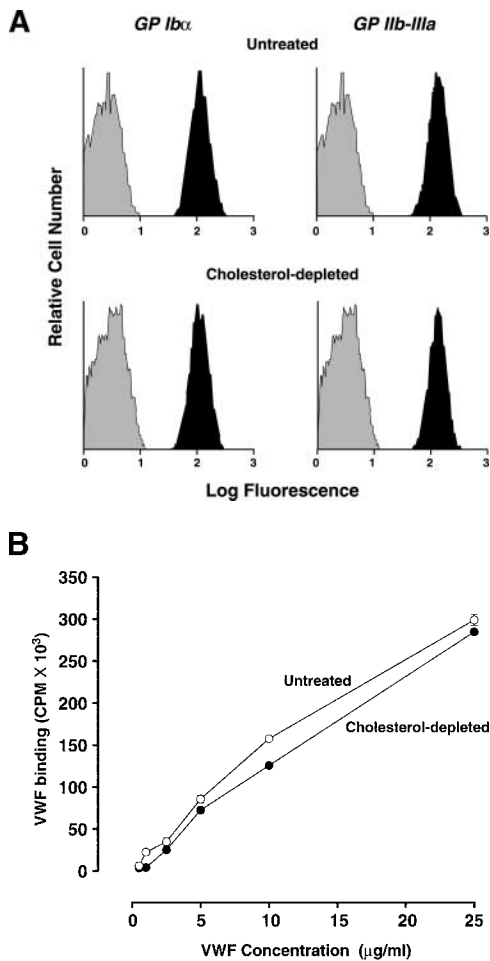


**Figure 7.** Cholesterol depletion does not affect platelet receptor levels or VWF binding. (A) The expression levels of the GP Ib-IX-V complex and the integrin  $\alpha_{\text{IIb}}\beta_3$  were compared in untreated and cholesterol-depleted washed platelets by staining with either FITC-conjugated anti-GP Ib $\alpha$  (SZ2) or anti- $\alpha_{\text{IIb}}\beta_3$  (P2) mAbs. The fluorescence of each sample was analyzed by flow cytometry (curves filled in black). The background fluorescence was set with a FITC-conjugated mouse IgG (gray). The results shown are representative of three separate experiments. (B)  $^{125}\text{I}$ -labeled VWF was incubated with washed untreated and cholesterol-depleted platelets in the presence of 1 mg/ml ristocetin. Specific binding was calculated by subtracting nonspecific binding measured in the presence of AK2, an antibody that blocks the GP Ib-VWF interaction. Data are expressed as the mean of triplicate samples ( $\pm$ SEM).

binding site for GP Ib $\alpha$ , but lacks the  $\alpha_{\text{IIb}}\beta_3$  binding site present in mature VWF.

The fact that the initial adhesive event precedes the generation of intracellular signals is supported by the demonstration that polystyrene beads coated with the ligand-binding region of GP Ib $\alpha$  can tether under flow to a surface of purified VWF (46). On platelets, however, the requirements for the complex to mediate adhesion are not as simple as merely the presence of the GP Ib $\alpha$  on the platelet surface. The fact that raft disruption has such a profound effect on GP Ib-IX-V-mediated adhesion to VWF suggests that the raft component of the complex has inherently different adhesive properties than the remaining complex

population, perhaps being organized into “adhesive patches” on the surface that are required for efficient platelet capture in flowing blood. Other adhesion receptors seem to function this way, their ability to mediate adhesion depending on their localization to specific regions of the plasma membranes of the cell on which they reside, although not necessarily to rafts. The leukocyte adhesion receptors L-selectin and PSGL-1, for example, both are found on the tips of leukocyte microvilli, and their location in these regions has been shown to facilitate their adhesive functions (47–49). Platelets do not have microvilli, but the partitioning of a subset of GP Ib-IX-V complexes to membrane microdomains may nevertheless facilitate adhesion. One possible mechanism would be by localizing the complex to a region of the membrane rich in signaling molecules that interact with the cytoplasmic domains and affect the ability of the extracellular portions to bind VWF.

Localization of the complex to lipid rafts appears to be a function of cysteine palmitoylation, a modification that may be dynamically regulated and thus amenable to pharmacological manipulation. Our studies showed that the raft fractions were greatly enriched in GP Ib-IX-V-associated palmitate, which increased with platelet activation (Fig. 2). Our use of octyl- $\beta$ -glucopyranoside during the immunoprecipitation procedure assured that the palmitate detected was associated with protein, but as yet we do not have definitive proof that the increase seen with VWF-mediated activation corresponds to increased GP Ib-IX-V complex palmitoylation. Another possibility is that other palmitoylated proteins associate noncovalently with the complex on VWF-mediated activation in a manner resistant to disruption by the detergents used. We are in the process of distinguishing between these two possibilities. If it turns out that the increase in GP Ib-IX-V-associated palmitoylation results from de novo attachment of palmitate to GP Ib $\beta$  and GP IX on VWF-induced platelet stimulation, this points to a role for regulated palmitoylation in platelet function and suggests the possibility that enzymatic acylation and deacylation of the GP Ib-IX-V complex may regulate its association with rafts and hence the VWF-induced platelet response.

These studies highlight a specific role for cholesterol in platelet function and raise the possibility that plasma cholesterol levels may modulate these functions. Consistent with this, several studies have shown that the lipid environment directly correlates with alterations in platelet cholesterol and function (50, 51). Early studies by Shattil and colleagues (52) demonstrated that cholesterol loading of platelets increased their reactivity to agonists and conversely, that cholesterol depletion had an inhibitory effect. More recent studies indicate that rafts are important in signaling from the collagen receptor GP VI (53–55), in cold activation of platelets (56), and for localizing production of phosphoinositide 3-kinase products (57). Since raft size depends on the concentration of sphingolipids and cholesterol in the membrane (58), it leads us to consider that the platelet hyperreactivity observed in high cholesterol disease states, such as hypercholesterolemia and atherosclerosis, may be attributable to increased raft function.



Thus, effects on platelet function via lipid rafts may be an important consequence of alteration in plasma lipid levels and could contribute to the morbidity associated with hypercholesterolemia, as well as being a salutary factor associated with lipid lowering.

The authors gratefully acknowledge Drs. Michael Berndt and Robert Andrews for their invaluable advice, and for kindly providing the WM23 and purified VWF. We also thank Gabriel Romo for the preparation of iodinated WM23 and VWF and for his technical assistance and Dr. Adam Munday for proof-reading the manuscript. We are also grateful to Jennifer Thaggard and Angela Bergeron for their technical assistance.

This work was supported by a National Institutes of Health Specialized Center of Research grant number P50HL65967.

Submitted: 28 January 2002

Revised: 25 June 2002

Accepted: 5 September 2002

## References

- Lopez, J.A. 1994. The platelet glycoprotein Ib-IX complex. *Blood Coagul. Fibrinolysis*. 5:97–119.
- Kroll, M.H., J.D. Hellums, L.V. McIntire, A.I. Schafer, and J.L. Moake. 1996. Platelets and shear stress. *Blood*. 88:1525–1541.
- Zaffran, Y., S.C. Meyer, E. Negrescu, K.B. Reddy, and J.E. Fox. 2000. Signaling across the platelet adhesion receptor glycoprotein Ib-IX induces  $\alpha_{IIb}\beta_3$  activation both in platelets and a transfected Chinese hamster ovary cell system. *J. Biol. Chem.* 275:16779–16787.
- Yap, C.L., S.C. Hughan, S.L. Cranmer, W.S. Nesbitt, M.M. Rooney, S. Giuliano, S. Kulkarni, S.M. Dopheide, Y. Yuan, H.H. Salem, and S.P. Jackson. 2000. Synergistic adhesive interactions and signaling mechanisms operating between platelet glycoprotein Ib/IX and integrin  $\alpha_{IIb}\beta_3$ . Studies in human platelets and transfected Chinese hamster ovary cells. *J. Biol. Chem.* 275:41377–41388.
- Kroll, M.H., T.S. Harris, J.L. Moake, R.I. Handin, and A.I. Schafer. 1991. von Willebrand factor binding to platelet GpIb initiates signals for platelet activation. *J. Clin. Invest.* 88:1568–1573.
- Ikeda, Y., M. Handa, T. Kamata, K. Kawano, Y. Kawai, K. Watanabe, K. Kawakami, K. Sakai, M. Fukuyama, I. Itagaki, et al. 1993. Transmembrane calcium influx associated with von Willebrand factor binding to GP Ib in the initiation of shear-induced platelet aggregation. *Thromb. Haemost.* 69:496–502.
- Razdan, K., J.D. Hellums, and M.H. Kroll. 1994. Shear-stress-induced von Willebrand factor binding to platelets causes the activation of tyrosine kinase(s). *Biochem. J.* 302: 681–686.
- Asazuma, N., Y. Ozaki, K. Satoh, Y. Yatomi, M. Handa, Y. Fujimura, S. Miura, and S. Kume. 1997. Glycoprotein Ib-von Willebrand factor interactions activate tyrosine kinases in human platelets. *Blood*. 90:4789–4798.
- Jackson, S.P., S.M. Schoenwaelder, Y. Yuan, I. Rabinowitz, H.H. Salem, and C.A. Mitchell. 1994. Adhesion receptor activation of phosphatidylinositol 3-kinase. von Willebrand factor stimulates the cytoskeletal association and activation of phosphatidylinositol 3-kinase and pp60c-src in human platelets. *J. Biol. Chem.* 269:27093–27099.
- Muszbeck, L., and M. Laposata. 1989. Glycoprotein Ib and glycoprotein IX in human platelets are acylated with palmitic acid through thioester linkages. *J. Biol. Chem.* 264:9716–9719.
- Yurchak, L.K., and B.M. Sefton. 1995. Palmitoylation of either Cys-3 or Cys-5 is required for the biological activity of the Lck tyrosine protein kinase. *Mol. Cell. Biol.* 15:6914–6922.
- Zhang, W., R.P. Tribble, and L.E. Samelson. 1998. LAT palmitoylation: its essential role in membrane microdomain targeting and tyrosine phosphorylation during T cell activation. *Immunity*. 9:239–246.
- Webb, Y., L. Hermida-Matsumoto, and M.D. Resh. 2000. Inhibition of protein palmitoylation, raft localization, and T cell signaling by 2-bromopalmitate and polyunsaturated fatty acids. *J. Biol. Chem.* 275:261–270.
- van't Hof, W., and M.D. Resh. 1999. Dual fatty acylation of p59(Fyn) is required for association with the T cell receptor  $\zeta$  chain through phosphotyrosine-Src homology domain-2 interactions. *J. Cell Biol.* 145:377–389.
- Melkonian, K.A., A.G. Ostermeyer, J.Z. Chen, M.G. Roth, and D.A. Brown. 1999. Role of lipid modifications in targeting proteins to detergent-resistant membrane rafts. Many raft proteins are acylated, while few are prenylated. *J. Biol. Chem.* 274:3910–3917.
- Simons, K., and E. Ikonen. 1997. Functional rafts in cell membranes. *Nature*. 387:569–572.
- Shenoy-Scaria, A.M., D.J. Dietzen, J. Kwong, D.C. Link, and D.M. Lublin. 1994. Cysteine3 of Src family protein tyrosine kinase determines palmitoylation and localization in caveolae. *J. Cell Biol.* 126:353–363.
- Brown, D.A., and J.K. Rose. 1992. Sorting of GPI-anchored proteins to glycolipid-enriched membrane subdomains during transport to the apical cell surface. *Cell*. 68:533–544.
- Brown, D.A., and E. London. 2000. Structure and function of sphingolipid- and cholesterol-rich membrane rafts. *J. Biol. Chem.* 275:17221–17224.
- Simons, K., and D. Toomre. 2000. Lipid rafts and signal transduction. *Nat. Rev. Mol. Cell Biol.* 1:31–39.
- Galbiati, F., B. Razani, and M.P. Lisanti. 2001. Emerging themes in lipid rafts and caveolae. *Cell*. 106:403–411.
- Janes, P.W., S.C. Ley, A.I. Magee, and P.S. Kabouridis. 2000. The role of lipid rafts in T cell antigen receptor (TCR) signalling. *Semin. Immunol.* 12:23–34.
- Cheng, P.C., M.L. Dykstra, R.N. Mitchell, and S.K. Pierce. 1999. A role for lipid rafts in B cell antigen receptor signaling and antigen targeting. *J. Exp. Med.* 190:1549–1560.
- Sheets, E.D., D. Holowka, and B. Baird. 1999. Membrane organization in immunoglobulin E receptor signaling. *Curr. Opin. Chem. Biol.* 3:95–99.
- Harder, T., P. Scheiffele, P. Verkade, and K. Simons. 1998. Lipid domain structure of the plasma membrane revealed by patching of membrane components. *J. Cell Biol.* 141:929–942.
- Janes, P.W., S.C. Ley, and A.I. Magee. 1999. Aggregation of lipid rafts accompanies signaling via the T cell antigen receptor. *J. Cell Biol.* 147:447–461.
- Stauffer, T.P., and T. Meyer. 1997. Compartmentalized IgE receptor-mediated signal transduction in living cells. *J. Cell Biol.* 139:1447–1454.
- Gouy, H., P. Deterre, P. Debre, and G. Bismuth. 1994. Cell calcium signaling via GM1 cell surface gangliosides in the human Jurkat T cell line. *J. Immunol.* 152:3271–3281.
- Andrews, R.K., J.J. Gorman, W.J. Booth, G.L. Corino, P.A. Castaldi, and M.C. Berndt. 1989. Cross-linking of a monomeric 39/34-kDa dispaase fragment of von Willebrand factor

- (Leu-480/Val-481-Gly-718) to the N-terminal region of the  $\alpha$ -chain of membrane glycoprotein Ib on intact platelets with bis(sulfosuccinimidyl) suberate. *Biochemistry*. 28:8326–8336.
30. Schulte, E.J., M.A. Cruz, J.B. Siegel, J. Anrather, and S.C. Robson. 1997. Activation of human platelets by the membrane-expressed A1 domain of von Willebrand factor. *Blood*. 90:4425–4437.
  31. Kowalska, M.A., L. Tan, J.C. Holt, M. Peng, J. Karczewski, J.J. Calvete, and S. Niewiarowski. 1998. Alboaggregins A and B. Structure and interaction with human platelets. *Thromb. Haemost.* 79:609–613.
  32. Andrews, R.K., M.H. Kroll, C.M. Ward, J.W. Rose, R.M.S. Carborough, A.I. Smith, J.A. Lopez, and M.C. Berndt. 1996. Binding of a novel 50-kilodalton alboaggregin from *Trimeresurus albolabris* and related viper venom proteins to the platelet membrane glycoprotein Ib-IX-V complex. Effect on platelet aggregation and glycoprotein Ib-mediated platelet activation. *Biochemistry*. 35:12629–12639.
  33. Navdaev, A., D. Dormann, J.M. Clemetson, and K.J. Clemetson. 2001. Echicetin, a GPIb-binding snake C-type lectin from *Echis carinatus*, also contains a binding site for IgM $\kappa$  responsible for platelet agglutination in plasma and inducing signal transduction. *Blood*. 97:2333–2341.
  34. Falati, S., C.E. Edmead, and A.W. Poole. 1999. Glycoprotein Ib-V-IX, a receptor for von Willebrand factor, couples physically and functionally to the Fc receptor  $\gamma$ -chain, Fyn, and Lyn to activate human platelets. *Blood*. 94:1648–1656.
  35. Sullam, P.M., W.C. Hyun, J. Szollosi, J. Dong, W.M. Foss, and J.A. Lopez. 1998. Physical proximity and functional interplay of the glycoprotein Ib-IX-V complex and the Fc receptor Fc $\gamma$ R1IA on the platelet plasma membrane. *J. Biol. Chem.* 273:5331–5336.
  36. Sun, B., J. Li, and J. Kambayashi. 1999. Interaction between GPIb $\alpha$  and Fc $\gamma$ RIIA receptor in human platelets. *Biochem. Biophys. Res. Commun.* 266:24–27.
  37. McNicol, A. 2001. Platelet preparation and estimation of functional responses. In *Platelets: A Practical Approach*. S.P. Watson and K.S. Authi, editors. Oxford University Press, New York. 1–26.
  38. Cruz, M.A., T.G. Diacovo, J. Emsley, R. Liddington, and R.I. Handin. 2000. Mapping the glycoprotein Ib-binding site in the von Willebrand factor A1 domain. *J. Biol. Chem.* 275:19098–19105.
  39. Berndt, M.C., C. Gregory, A. Kabral, H. Zola, D. Fournier, and P.A. Castaldi. 1985. Purification and preliminary characterization of the glycoprotein Ib complex in the human platelet membrane. *Eur. J. Biochem.* 151:637–649.
  40. Dorahy, D.J., L.F. Lincz, C.J. Meldrum, and G.F. Burns. 1996. Biochemical isolation of a membrane microdomain from resting platelets highly enriched in the plasma membrane glycoprotein CD36. *Biochem. J.* 319:67–72.
  41. Mazzucato, M., L. De Marco, P. Pradella, A. Masotti, and F.I. Pareti. 1996. Porcine von Willebrand factor binding to human platelet GPIb induces transmembrane calcium influx. *Thromb. Haemost.* 75:655–660.
  42. Pareti, F.I., M. Mazzucato, E. Bottini, and P.M. Mannucci. 1992. Interaction of porcine von Willebrand factor with the platelet glycoproteins Ib and IIb/IIIa complex. *Br. J. Haematol.* 82:81–86.
  43. Kilsdonk, E.P., P.G. Yancey, G.W. Stoudt, F.W. Bangerter, W.J. Johnson, M.C. Phillips, and G.H. Rothblat. 1995. Cellular cholesterol efflux mediated by cyclodextrins. *J. Biol. Chem.* 270:17250–17256.
  44. Torti, M., A. Bertoni, I. Canobbio, F. Sinigaglia, E.G. Lapetina, and C. Balduino. 1999. Rap1B and Rap2B translocation to the cytoskeleton by von Willebrand factor involves Fc $\gamma$ RII receptor-mediated protein tyrosine phosphorylation. *J. Biol. Chem.* 274:13690–13697.
  45. Canobbio, I., A. Bertoni, P. Lova, S. Paganini, E. Hirsch, F. Sinigaglia, C. Balduino, and M. Torti. 2001. Platelet activation by von Willebrand factor requires coordinated signaling through thromboxane A2 and Fc  $\gamma$  IIA receptor. *J. Biol. Chem.* 276:26022–26029.
  46. Marchese, P., E. Saldivar, J. Ware, and Z.M. Ruggeri. 1999. Adhesive properties of the isolated amino-terminal domain of platelet glycoprotein Ib $\alpha$  in a flow field. *Proc. Natl. Acad. Sci. USA*. 96:7837–7842.
  47. Moore, K.L., K.D. Patel, R.E. Bruehl, F. Li, D.A. Johnson, H.S. Lichenstein, R.D. Cummings, D.F. Bainton, and R.P. McEver. 1995. P-selectin glycoprotein ligand-1 mediates rolling of human neutrophils on P-selectin. *J. Cell Biol.* 128:661–671.
  48. Bruehl, R.E., K.L. Moore, D.E. Lorant, N. Borregaard, G.A. Zimmerman, R.P. McEver, and D.F. Bainton. 1997. Leukocyte activation induces surface redistribution of P-selectin glycoprotein ligand-1. *J. Leukoc. Biol.* 61:489–499.
  49. von Andrian, U.H., S.R. Hasslen, R.D. Nelson, S.L. Erlandsen, and E.C. Butcher. 1995. A central role for microvillous receptor presentation in leukocyte adhesion under flow. *Cell*. 82:989–999.
  50. Tandon, N.N., J.M. Hoeg, and G.A. Jamieson. 1985. Perfusion studies on the formation of mural thrombi with cholesterol-modified and hypercholesterolemic platelets. *J. Lab. Clin. Med.* 105:157–163.
  51. Quan Sang, K.H., M. Mazeaud, C. Astarie, V. Duranthon, F. Driss, and M.A. Devynck. 1993. Plasma lipids and platelet membrane fluidity in essential hypertension. *Thromb. Haemost.* 69:70–76.
  52. Shattil, S.J., R. Anaya-Galindo, J. Bennett, R.W. Colman, and R.A. Cooper. 1975. Platelet hypersensitivity induced by cholesterol incorporation. *J. Clin. Invest.* 55:636–643.
  53. Locke, D., H. Chen, Y. Liu, C. Liu, and M.L. Kahn. 2002. Lipid rafts orchestrate signaling by the platelet receptor glycoprotein VI. *J. Biol. Chem.* 277:18801–18809.
  54. Ezumi, Y., K. Kodama, T. Uchiyama, and H. Takayama. 2002. Constitutive and functional association of the platelet collagen receptor glycoprotein VI-Fc receptor  $\gamma$ -chain complex with membrane rafts. *Blood*. 99:3250–3255.
  55. Wonerow, P., A. Obergfell, J.I. Wilde, R. Bobe, N. Asazuma, T. Brdicka, A. Leo, B. Schraven, V. Horejsi, S.J. Shattil, and S.P. Watson. 2002. Differential role of glycolipid-enriched membrane domains in glycoprotein VI- and integrin-mediated phospholipase C $\gamma$ 2 regulation in platelets. *Biochem. J.* 364:755–765.
  56. Gousset, K., W.F. Wolkers, N.M. Tsvetkova, A.E. Oliver, C.L. Field, N.J. Walker, J.H. Crowe, and F. Tablin. 2002. Evidence for a physiological role for membrane rafts in human platelets. *J. Cell. Physiol.* 190:117–128.
  57. Bodin, S., S. Giuriato, J. Ragab, B.M. Humbel, C. Viala, C. Vieu, H. Chap, and B. Payastre. 2001. Production of phosphatidylinositol 3,4,5-trisphosphate and phosphatidic acid in platelet rafts: evidence for a critical role of cholesterol-enriched domains in human platelet activation. *Biochemistry*. 40:15290–15299.
  58. Simons, K., and E. Ikonen. 2000. How cells handle cholesterol. *Science*. 290:1721–1726.